J. Mater. Environ. Sci. 3 (2) (2012) 360-373
ISSN : 2028-2508
CODEN: JMESCN

Corrosion inhibition of Al-Mg alloy in hydrochloric acid using Benzylamine-N-(p-methoxy benzylidene)

V.A. Panchal[#], A.S. Patel, P.T. Trivedi, N.K. Shah*
Department of Chemistry, School of Sciences, Gujarat University, Ahmedabad-09, Gujarat, India.

Received 4 Oct 2011, Revised 21 Dec 2011, Accepted 21 Dec 2011.
* Corresponding author. nishchem2004@yahoo.co.in**;** Tel No. (O) : +91-079-26305037

Abstract
Corrosion inhibition of Al-Mg alloy in 2.0 M HCl was investigated in the absence and presence of different concentration of Benzylamine-N-(p-methoxy benzylidene) [BANPMB]. Weight loss, galvanostatic polarization, electrochemical impedance spectroscopy (EIS) and scanning electron microscopy (SEM) were employed. The inhibition efficiency increased with increase in inhibitor concentration but decreased with increase in temperature. The adsorption of Schiff base was found to obey Langmuir adsorption isotherm. Some thermodynamic parameters (ΔG_{ads} and Q_{ads}) and activation energy (E_a) were calculated to elaborate the mechanism of corrosion inhibition. The polarization measurement indicated that the inhibitor is of mixed type. Electrochemical impedance was used to investigate the mechanism of corrosion inhibition. The surface characteristics of inhibited and uninhibited metal samples were investigated by scanning electron microscopy (SEM).

Keywords : Al-Mg alloy; Corrosion inhibition; HCl; EIS; SEM

1. Introduction
Corrosion of metal is caused by electrochemical reaction between a metal (or an alloy) and aqueous phase. It proceeds according to a complex electrochemical process that is related to the atomic structure of matter. The corrosion of metal is the result of two simultaneous reactions that are in electrical equilibrium, i.e., oxidation of metal to metal ions and reduction of hydrogen to hydrogen gas. Aluminum and its alloys have low density, attractive appearance, relatively good corrosion resistance and excellent thermal and electrical conductivity. The combination of these properties makes it a preferred choice for many industrials applications such as automobiles, food handling, containers, electronic devices, buildings, aviations, etc. [1-3]. Various attempts have been made to study the corrosion inhibition by organic inhibitors in acid solutions [4-8].

Hydrochloric acid and sulphuric acid solutions are used for pickling of aluminium or for its chemical or electrochemical etching. It is very important to add corrosion inhibitors to decrease the rate of metal dissolution in such solutions. The inhibition of aluminium and its alloys in acidic solutions were extensively studied using organic compounds [9-16]. It is known that the organic compounds are effective corrosion inhibitors due to their ability to form an adsorbed protective film at the metal surface. The adsorption of the

surfactant on the metal surface can markedly change the corrosion resisting properties of the metals [17, 18]. So the study of the relations between the adsorption and corrosion inhibition is of great importance.

Some Schiff bases have recently reported as effective corrosion inhibitors in acidic media for steel [19, 20], aluminium [21], aluminium alloys [22,23] and copper [24]. Due to the presence of the > C = N – group, electronegative nitrogen, sulfur and/or oxygen atoms in the molecules, Schiff bases should be good corrosion inhibitors. The action of such inhibitors depends on the specific interaction between the functional groups and the metal surface. So it is very important to clarify the interactions between inhibitor molecules and metal surfaces in order to search new and efficient corrosion inhibitors [25-28].

In earlier work the inhibition of corrosion of zinc in sulphuric acid by Schiff bases of ethylenediamine [29], ortho-substituted aniline-N-salicylidenes [30], ortho-, meta-, and para-aminophenol-N-salicylidenes [31], meta-substituted aniline-N-salicylidenes [32] and Salicylidene-N-N'-morpholine [33] have been reported.

In the present work, the inhibitive effectiveness of BANPMB have been studied in retarding corrosion of Al-Mg alloy in 2.0 M HCl. Weight loss method, galvanostatic polarization, electrochemical impedance spectroscopy (EIS) and scanning electron microscopy (SEM) techniques were used to investigate the inhibiting influence of BANPMB. EIS has been considered as a valuable and powerful tool to assess the degradation of organic coatings [34]. EIS has long been used to predict the service lifetime of corrosion protective layers. EIS data are also assimilated to develop meaningful models to analysis the physical behavior of the coating degradation [35]. Scanning electron microscopy (SEM) was employed to observe the surface morphology of the mild steel corroded in test solutions [36].

2. Experimental

2.1 Synthesis of Schiff base

Schiff base used in the present work was synthesized from equimolar amount of p-methoxy benzaldehyde and Benzylamine through a condensation reaction in ethanol media as prescribed by Shah et al. [37]. BANPMB [registry number:-622-72-0, color:-dark yellowish liquid, b.p.:- 225.1°C, 0.5268 mW/mg from DSC graph (Fig.1)] is insoluble in water but soluble in ethanol. The compound was characterized through its structure data [IR (Fig.2)] and its purity was confirmed by thin-layer chromatography (TLC). The chemical structure of the investigated compound is given below :

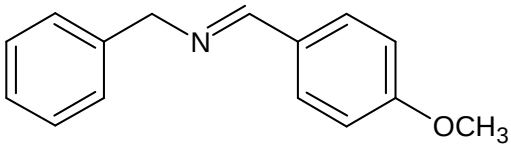

BANPMB

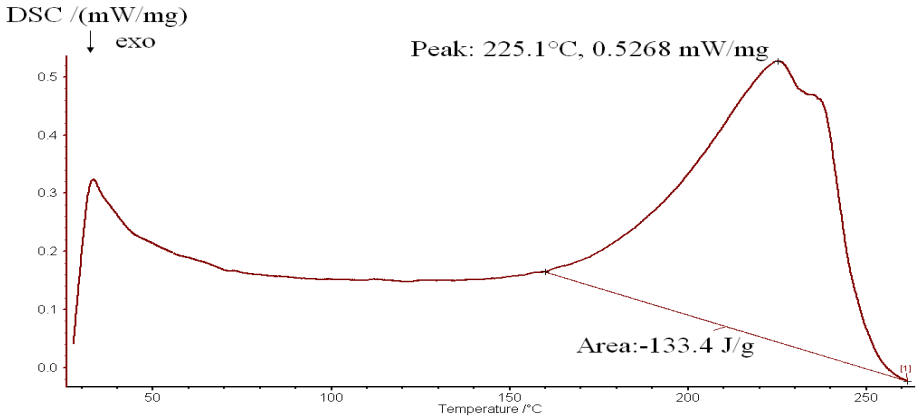

Fig.1 DSC graph of BANPMB

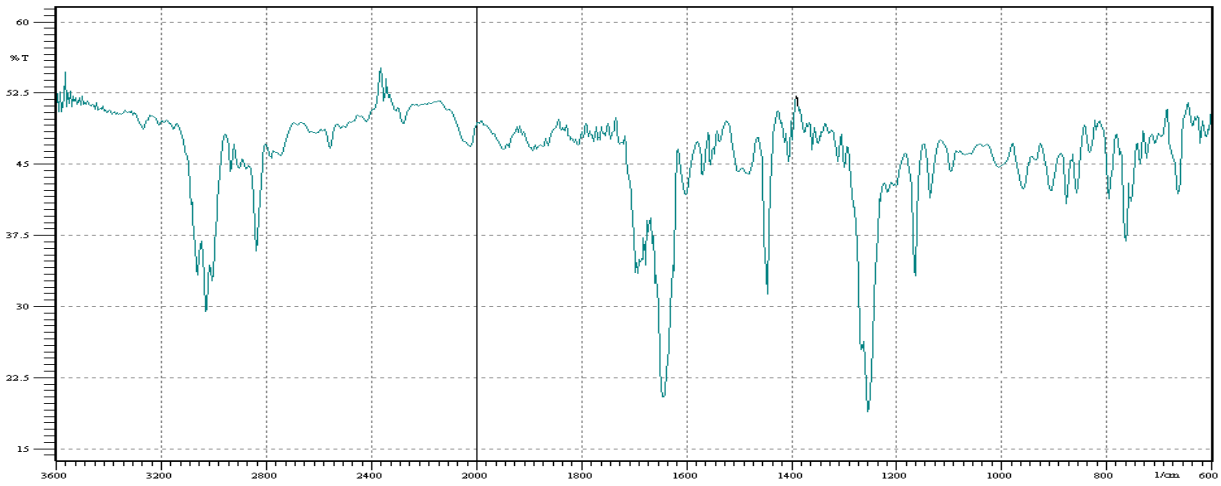

aromatic ring :- 3080 cm^{-1}, >C=N- :- 1647 cm^{-1}, -C-OCH_3 :- 1258 cm^{-1}

Fig. 2 : IR Spectrum of BANPMB.

2.2 Electrodes and electrolytes:

Corrosion test were performed using coupons prepared from Al-Mg alloy. The chemical composition (wt%) of the Al-Mg alloy sample is Mg(2.6%), Cu(0.1%), Si(0.6%), Fe(0.5%), Mn(0.5%), Cr(0.4%) and balance Al. Rectangular specimens of Al-Mg alloy of size 6 cm × 3 cm and thickness 0.087 cm with a small hole of about 2 mm diameter just near the upper end of the specimen were used for the determination of weight loss. The specimens were polished with '0', '00', '000' and '0000' grade Oakey emery paper. The specimens degreased by A. R. carbon tetrachloride (sulphur free).

For polarization and impedance measurements, metal coupons of circular design, diameter 2.802 cm with a handle 3 cm long and 0.5 cm wide and thickness 0.087 cm with a small hole of about 2 mm diameter just near the upper end of the specimen were used. The handle and the back of the coupon and of the auxiliary platinum electrode were coated with Perspex leaving only the circular portion of the specimen of apparent surface area 6.156 cm^2 exposed to the solution.

The corrosive solution (2.0 M HCl) was prepared by dilution of analytical grade 37% HCl (NICE) with double distilled water. The concentration range of employed inhibitor was 0.001 to 0.5% in 1.0 M HCl. The used all chemicals for preparation of Schiff base were AR grade (MERCK).

2.3 Measurements:

Three methods namely weight loss method, impedance spectroscopy, polarization study and scanning electron microscopy were used to determine the corrosion inhibition efficiencies of BANPMB.

2.3.1 Weight loss method:

In weight loss method, the specimens were exposed to 2.0 M HCl solution containing controlled addition of BANPMB in the range of 0.001% to 0.5% inhibitor concentration. One specimen only was suspended by a glass hook in each beaker containing 230 ml of the test solution which was open to the air at 35° ± 0.5°C, to the same depth of about 1.5cm below the surface of the test solution. The experiments were repeated at different temperatures, ranging from 35° ± 0.5°C to 65° ± 0.5°C in absence and presence of 0.5% inhibitor's concentration after 30 minutes.

2.3.2 Electrochemical measurements:

Electrochemical experiments were carried out using a standard electrochemical three-electrode cell. Al-Mg alloy was used as working electrode, platinum as counter electrode and saturated calomel electrode (SCE) as reference electrode. The test solution was contained in a H-type (80 ml in each limb) Pyrex glass cell with Luggin capillary as near to the electrode surface as possible and a porous partition to separate the two compartments. The potential was measured against a saturated calomel electrode (SCE), in polarization study.

The corrosion parameters such as corrosion potential (E_{corr}), corrosion current density (I_{corr}) and Tafel plots were measured in polarization method. In this study, the current density was varied in the range of 2×10^{-4} to 3.25×10^{-2} A cm^{-2}.

Electrochemical impedance measurements were carried out in the frequency range of 20 kHz – 0.1 Hz at the open circuit potential, after 30 minutes of immersion, by applying amplitude of 5 mV sine wave ac signal (AUTOLAB). Double layer capacitance (C_{dl}) and charge transfer resistance (R_{ct}) values were calculated from Nyquist plots as described by Hosseini [38]. EIS data were analyzed using frequency response analyzer (FRA) electrochemical setup.

2.3.3. Scanning electron microscopic studies:

The surface morphology of the Al-Mg alloy samples in absence and presence of BANPMB was investigated after weight loss using SEM technique [Make/model LEO 1430 VP]. The SEM images with magnification 20 μm and 50 μm of the metal surfaces after weight loss were taken.

3. Results and Discussion

3.1 Weight loss method

3.1.1 Effect of inhibitor concentration

The corrosion rate of Al-Mg alloy in absence and presence of BANPMB at 35° ± 0.5°C were studied using weight loss method. Table-1 shows that the calculated values of inhibition efficiency (%IE) and surface coverage (θ) for Al-Mg alloy dissolution in 2.0 M HCl in absence and presence of BANPMB. The results show that inhibitor actually inhibited the corrosion of Al-Mg alloy in 2.0 M HCl solutions. The inhibition efficiency was found to be depended on the concentration of the inhibitor. As the concentration of the inhibitor increases, the inhibition efficiency (%IE) is going up to a maximum values. The inhibitory action of the inhibitor against Al-Mg alloy corrosion can be attributed to the adsorption of Schiff base molecules on the Al-Mg alloy surface, which limits the dissolution of the latter by blocking it corrosion sites and hence decreasing the weight loss, with increasing efficiency as the concentration increases. Similar reports have been documented elsewhere [39, 40].

Table-1 Corrosion parameters for Al-Mg alloy in the presence and absence of different concentrations of BANPMB obtained from weight loss measurement at 35°C ± 0.5°C for exposure period of 30 minutes.

Inhibitor	Concentration (%v/v)	Weight loss (mg dm^{-2})	Surface coverage (θ)	(%IE)
Blank	-	1120	-	-
BANPMB	0.001	487	0.565	56.5
	0.01	295	0.737	73.7
	0.05	181	0.838	83.8
	0.10	106	0.905	90.5
	0.50	11	0.990	99.0

The inhibition efficiency (%IE) and degree of surface coverage (θ) were calculated using equations 1 and 2, respectively [41]:

$$\text{Inhibition efficiency (\%IE)} = \frac{W_u - W_i}{W_u} \text{ X } 100 \quad \text{..... (1)}$$

$$\text{Surface coverage } (\theta) = \frac{W_u - W_i}{W_u} \quad \text{.....(2)}$$

Where W_u and W_i are the weight loss of Al-Mg alloy in 2.0 M HCl in absence and presence of BANPMB.

3.1.2. Adsorption behavior

It is generally assumed that the adsorption of the inhibitor at the metal/solution interface is the first step in the mechanism of inhibition in aggressive media. Two main types of interaction can describe the adsorption of inhibition namely : 1) Physical adsorption, 2) Chemical adsorption. In view of the above discussion, two modes of adsorption, physisorption and chemisorption, should be considered. The proceeding of physical adsorption requires the presence of electrically charged metal surface and charged species in the bulk of the solution [42]. While chemical adsorption process involved charge sharing or charge transfer from the inhibitor molecules to the vacant p-orbital in Al surface [42].

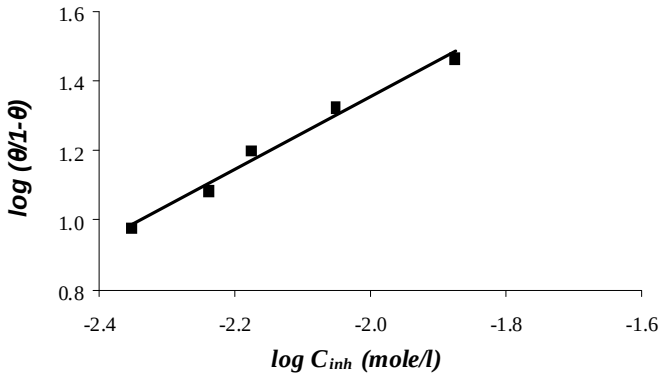

Fig. 3 : Langmuir isotherm for adsorption of Schiff base on the Al-Mg alloy metal surface.

The extent of corrosion inhibition depends on the surface conditions and the mode of adsorption of the inhibitors [43], under the assumptions that the corrosion of the covered parts of the surface is equal to zero and that corrosion takes place only on the uncovered parts of the surface. Basic information on the interaction between the organic compounds and metal surface can be provided from the adsorption isotherms. The values of surface coverage (θ) for the different concentration of the studied compound at 35 ± 0.5°C have been sued to explain the best adsorption isotherm to determine the adsorption process. The surface coverage values were calculated from Eq. 2 and shows in Table-1.

Several adsorption isotherms (Langmuir isotherm, Frundlich isotherm and Temkin isotherm) were tested for the description of adsorption behavior of studied compound and it is found that adsorption of studied Schiff base on Al-Mg alloy surface in HCl solution obey the Langmuir adsorption isotherm given by Eq. 3

$$C_{inh} = \frac{\theta}{K(1 - \theta)} \quad \text{.....(3)}$$

Where, C_{inh} is the inhibitor concentration, θ is the surface coverage values and K is the equilibrium constants of adsorption process. Thus, these results suggest that there are no interaction or repulsion forces between the adsorbed molecules. Typical plot of log (θ/1-θ) vs log C_{inh} for BANPMB is given in Fig. 3. It is also indicating that the formation of a monolayer adsorbate film on the Al-Mg alloy surface.

3.1.3. Effect of temperature

The temperature could affect the interaction between the metal surface and acidic media in absence and presence of BANPMB. The effect of temperature on the inhibition efficiency for Al-Mg alloy in 2.0 M HCl solution in absence and presence of inhibitor (0.5% BANPMB) at temperature ranging from 35 to 65°C was obtained by weight loss measurements. The results are also given in Table-2.

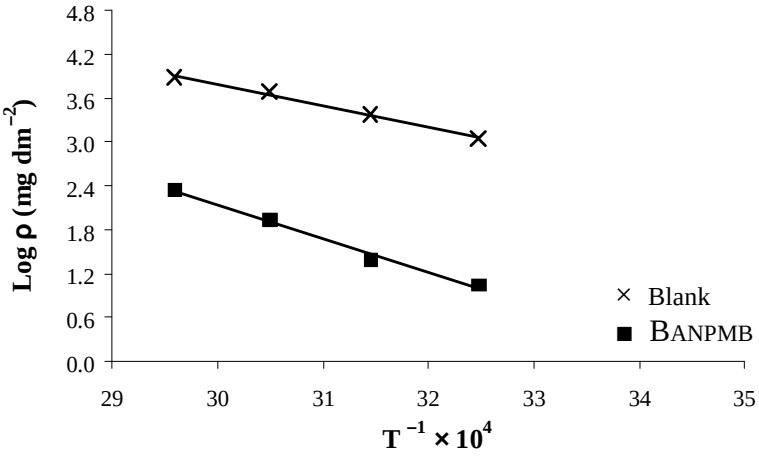

Fig. 4 : log ρ vs. $T^{-1} \times 10^4$ to calculate the activation energy of corrosion process in presence and absence of BANPMB.

The inhibition efficiencies are found to decrease with increasing the solution temperature from 35°C to 65°C. The decrease in inhibition efficiency shows that the film formed on the metal surface is less protective at higher temperature, i.e., the desorption rate of the inhibitor is greater at higher temperature [44].

Table-2 Temperature effect on the weight loss and inhibition efficiency for Al-Mg alloy in 2.0 M hydrochloric acid.

Inhibitor	Concentration (% v/v)	Weight loss (mg dm^{-2}) at temperature			
		35^o C	45^o C	55^o C	65^o C
Blank	-	1120	2399	4910	7608
BANPMB	0.5	11 (99.0%)	24 (99.0%)	85 (98.3%)	223 (97.1%)

3.1.4. Thermodynamic parameters

In acidic solution the corrosion rate is related to temperature by Arrhenius equation (4) [45],

$$\rho = k \exp\left(-E_a / RT\right) \quad \text{.....(4)}$$

Where, ρ is corrosion rate determined from the weight loss measurement, E_a is the apparent activation energy, A is the Arrhenius constant, R is the molar gas constant and T is the absolute temperature. The apparent activation energy was determined from the slopes of log ρ versus $1/T \times 10^4$ graph depicted in Fig. 4. The values of activation energies were calculated and given in Table-3. These values indicate that the presence of BANPMB increases the activation energy of the metal dissolution reaction. The adsorption of the inhibitor is assumed to occur on the higher energy sites and the presence of the inhibitor, which results in the blocking of the active sites, must be associated with an increase in the activation energy of metal corrosion in the inhibited state [46]. The higher values of E_a in the presence of BANPMB compared to that in its absence and

the decrease in the inhibition efficiency (%IE) with rise in temperature is interpreted as an indication of physisorption [47, 48].

If it is assumed that the inhibitor is adsorbed on the metal surface in the form of a monolayer film, covering at any instant a fraction, θ, of the metal surface in a uniform random manner, then the heat of adsorption (Q_{ads}) of the inhibitor can be calculated from equation 5:

$$(Q_{ads}) = 2.303R \left\{ \log \frac{\theta_2}{1-\theta_2} - \log \frac{\theta_1}{1-\theta_1} \right\} \left(\frac{T_1 T_2}{T_2 - T_1} \right) \quad \text{.....(5)}$$

Where, θ_1 and θ_2 are the values of surface coverage at temperature T_1 and T_2, respectively.
The values of the free energy of adsorption (ΔG_{ads}) were calculated from equations 6 and 7 [49]

$$\log C_{inh} = \log \frac{\theta}{1-\theta} - \log B \quad \text{..... (6)}$$

$$\text{where, } \log B = -1.74 - [\ \Delta Gads / 2.303RT\ ] \quad \text{.....(7)}$$

The values of ΔG_{ads} and Q_{ads} are shown in Table-3. The values of ΔG_{ads} are negative, indicating that the adsorption of inhibitor molecules on the metal surface is spontaneous process. The studied inhibitor obeys the general rule that the effectiveness of corrosion inhibition increases with increasing the negative values of ΔG_{ads}.

Table-3 Thermodynamic parameters and activation energy for inhibitor adsorption for corrosion of Al-Mg alloy in 2.0 M HCl.

Inhibitor	E_a (kJ mole^{-1})	Q_{ads} (kJ mole^{-1})	ΔG_{ads} (kJ mole^{-1})
Blank	59.8	-	-
BANPMB	87.9	-34.3	-32.1

Generally, values of ΔG_{ads} around –20 kJ mole^{-1} or lower are consistent with the electrostatic interaction between charged molecules and the charged metal surface (physisorption), those around –40 kJ mole^{-1} or higher involves charge sharing or transfer from organic molecules to the metal surface is form a coordinate type of metal bond (chemisorption) [50]. The calculated ΔG_{ads} values are almost slightly less negative than –40 kJ mole^{-1}, indicating that the adsorption of inhibitor is not meanly physisorption or chemisorption but obeys comprehensive adsorption (physical and chemical adsorption). In addition, limited decrease in the absolute value of ΔG_{ads} with an increase in the temperatures, indicating that the adsorption was somewhat unfavorable with increasing experimental temperature, indicating that physisorption has the major contribution while chemisorption has the minor contribution in the adsorption mechanism.

The negative value of the heat of adsorption (Q_{ads}) indicates that the adsorption process is exothermic in nature. This observation further confirms physical adsorption of the inhibitor on the metal surface in HCl solution.

3.2 Electrochemical impedance spectroscopy (EIS)

The corrosion of Al-Mg alloy in 2.0 M HCl solution in absence and presence of BANPMB was investigated by EIS at the open circuit potential condition. The effects of the inhibitor concentration on the impedance behavior of metal in 2.0 M HCl have been studied and the corresponding Nyquist plots are given in Fig.5.

The Nyquist diagram obtained with 2.0 M HCl shows capacitive loop and the diameter of the semicircle increases on increasing the inhibitor concentration suggesting that the formed inhibitive film was strengthened by the addition of inhibitor. All the obtained plots show only one semicircle and they were fitted using equivalent circuit model (Fig.6) with capacitance (C) and resistance (R). The charge transfer resistance

(R_{ct}) values were calculated from the difference in impedance at lower and higher frequencies as suggested by Tsuru et. al. [51]. To obtain the double layer capacitance (C_{dl}) the frequency at which the imaginary component of the impedance is maximal ($-Z''_{max}$) was found as represented as following equation,

$$C_{dl} = Yo(\omega_{max})^{n-1} \quad \text{..... (8)}$$

All the impedance parameters [Double layer capacitance (C_{dl}), Charge transfer resistance (R_{ct}), Solution resistance (R_s)] are derived from Nyquist plots and the inhibition efficiency (%IE) is given in Table 4.

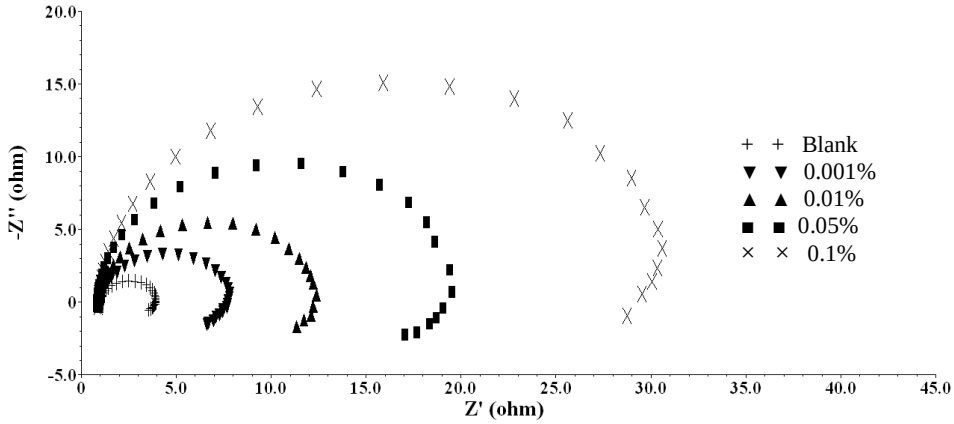

Fig. 5 : Impedance plot obtained at 35ºC in 2.0 M HCl in various concentration of BANPMB.

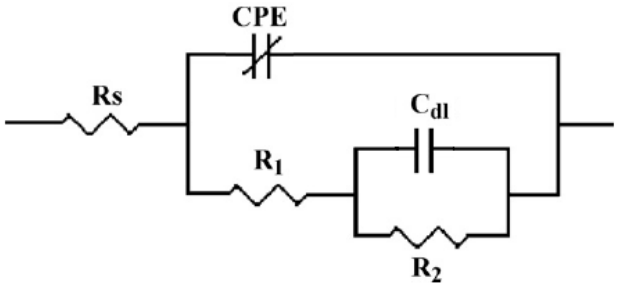

Fig. 6 : The equivalent circuit model (Randle's model) used to fit the experimental result.

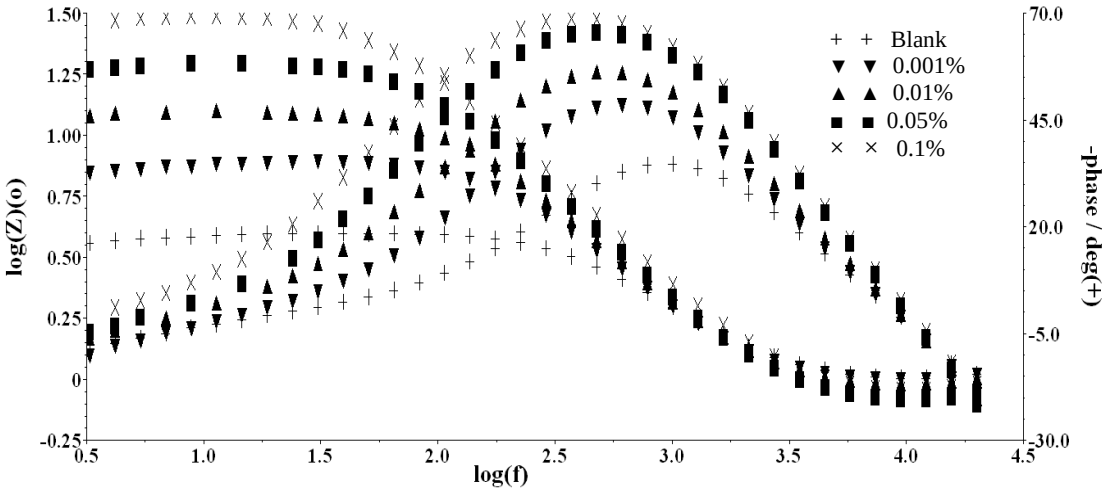

Fig. 7 : Bode plots obtained at 35ºC in 2.0 M HCl in various concentration of BANPMB.

The %IE at different inhibitor concentration were calculated by using equation 9:

$$\text{Inhibition Efficiency (\%IE)} = \frac{R\,ct - R^{o}\,ct}{R\,ct} \times 100 \quad \text{.....(9)}$$

where, R_{ct} and R°_{ct} are the charge transfer resistance in the HCl solution in the presence and absence of BANPMB, respectively. The corresponding Bode plots are show in Fig.7.

Table-4 Impedance parameters and corresponding inhibition efficiency for the corrosion of Al-Mg alloy in the 2.0 M HCl.

Inhibitor	Concentration	R_s (ohm)	R_{ct} (ohm)	C_{dl} (µF)	(%IE)
Blank	-	1.036	2.89	109.7	-
BANPMB	0.001	1.024	6.80	107.9	57.4
	0.01	0.970	11.25	100.7	74.2
	0.05	0.833	18.96	98.18	84.7
	0.10	0.912	30.12	84.39	90.4

The lower capacitance (C_{dl}) values for 2.0 M HCl medium indicates the inhomogeneity of surface of the metal roughened due to corrosion. The C_{dl} values decreases on increasing the inhibitor concentration and reaches very low value for the optimum concentration of all the studied systems indicating that the reduction of charges accumulated in the double layer due to formation of adsorbed inhibitor layer [52]. The charge transfer resistance (R_{ct}) of double layer increases with increasing the concentration of the inhibitor upto the optimum level indicating the decreased corrosion rate. In this case, R_s values can be neglected because of the value is small as compare to that of the values of R_{ct} and C_{dl}.

3.3 Galvanostatic polarisation

Fig.8 show polarization curves of Al-Mg alloy surface in 2.0 M HCl in the presence and absence of BANPMB. As would be expected both anodic and cathodic reactions of metal surface corrosion were inhibited with the increase of inhibitor concentration. This result suggests that the addition of BANPMB reduces a little bit anodic dissolution and significant retards the hydrogen evolution reaction [53]. So this inhibitor is a mixed type inhibitor with predominantly effect on the cathode.

Table-5 shows that the electrochemical corrosion kinetics parameters, i.e., corrosion potential (E_{corr}), cathodic and anodic slopes (b_c, b_a) and corrosion current density (I_{corr}) obtained by extrapolation of the Tafel lines. The calculated inhibition efficiency (%IE) is also reported from equation 10:

$$\text{Inhibition Efficiency (\%IE)} = \frac{I^{o}\,corr - Icorr}{I^{o}\,corr} \times 100 \quad \text{.....(10)}$$

Where, I°_{corr} and I_{corr} are uninhibited and inhibited corrosion current density, respectively.

Table-5 Electrochemical parameters of corrosion of Al-Mg alloy in the presence of different concentration of BANPMB at 35ºC and corresponding inhibition efficiencies obtained from polarization method.

Inhibitor	Concentration	E_{corr} (mV)	b_a (mV/dec)	b_c (mV/dec)	I_{corr} for cathodic (A cm^{-2})	(%IE)
Blank	-	-851	113	121	6.309×10^{-3}	-

BANPMB	0.001	-862	129	145	1.905×10^{-3}	69.8
	0.05	-877	132	131	5.754×10^{-4}	90.9

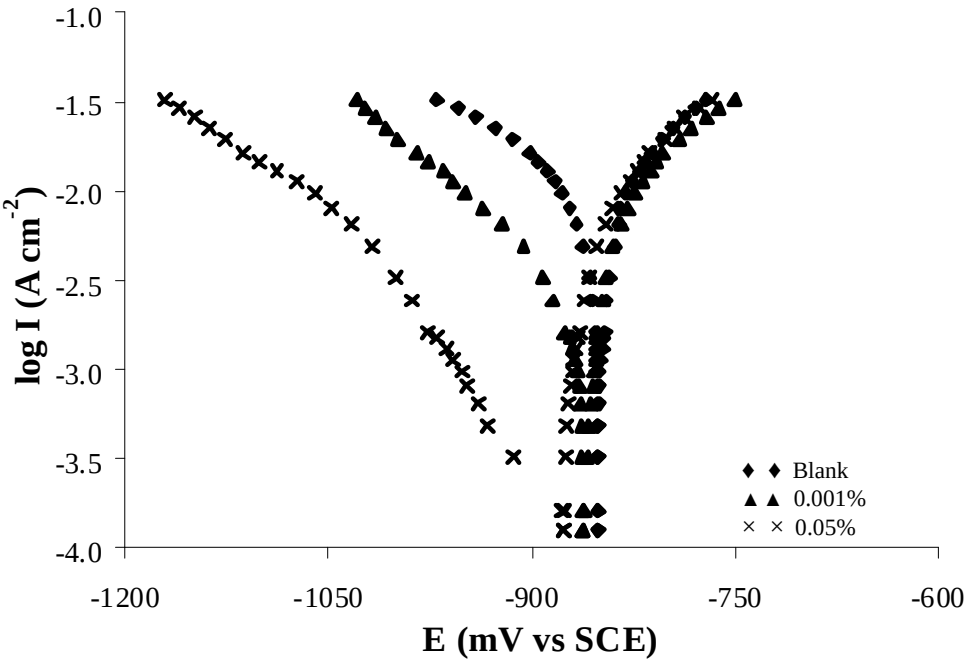

Fig. 8 : Anodic and cathodic polarization curves obtained for Al-Mg alloy metal at 35°C ± 0.5°C in 2.0 M HCl in various concentration of studied Schiff base ANPMB.

The good inhibition efficiency was about 83% for BANPMB at 0.5%. It can be seen that by increasing the inhibitor concentration, the corrosion rate decreased while the inhibition efficiency (%IE) increased. The addition of BANPMB decreases the I_{corr} values significantly for all the studied concentrations (0.001% and 0.05%) due to the increase in blocked fraction of metal surface by adsorption. It is also evident from this study that the inhibition of Al-Mg alloy corrosion is under both cathodic and anodic control therefore inhibitor can be classified as a mixed type inhibitor. The Tafel slope variations suggest that Schiff base influence the kinetics of the hydrogen evolution reaction.

No definite trend was observed in the shift of E_{corr} values, in presence of various concentration of BANPMB, suggesting that this compound behave as mixed type inhibitor. Moreover, the inhibitor causes no change in the anodic and cathodic Tafel slopes, indicating that the inhibitor is first adsorbed onto metal surface and therefore, impedes by merely blocking the reaction sites of metal surface without affecting the anodic and cathodic reaction mechanism [54].

3.4 Scanning electron microscopy (SEM)

The surface morphology of Al-Mg alloy specimens exposed to 2.0 M HCl solution in absence and presence of BANPMB for 30 minutes was examined by high resolution SEM technique. Fig.9 shows SEM images of Al-Mg alloy surface which immersed in 2.0 HCl solutions with and without the addition of 0.5% of BANPMB. It can be clear that the specimen surface was strongly damaged in absence of inhibitor due to metal dissolution in aggressive solution. A large number of pits with large size and high depth distributed over the

surface are seen (Fig.9c & 9d). However, no pits and cracks were observed in the micrograph after the addition of inhibitor to the aggressive solution (Fig.9a & 9b). Inhibitor molecules adsorbed on active sites of Al-Mg alloy and a smoother surface was observed when compared to the surface treated with uninhibited 2.0 M HCl solution.

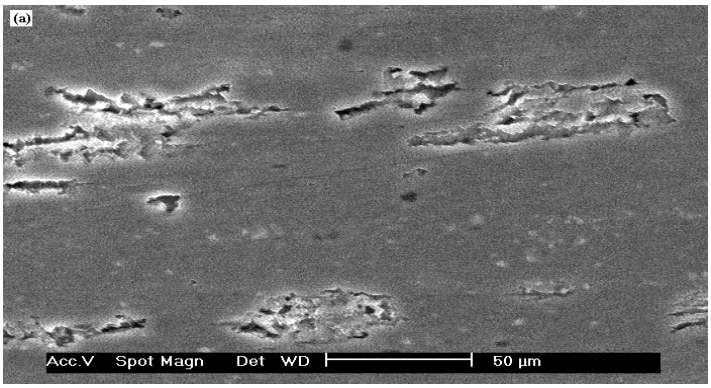

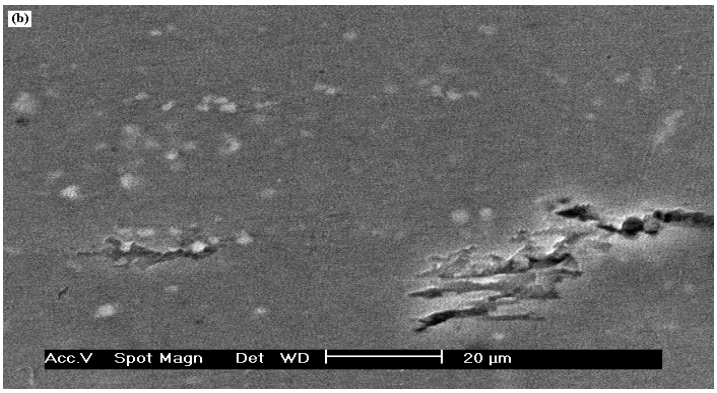

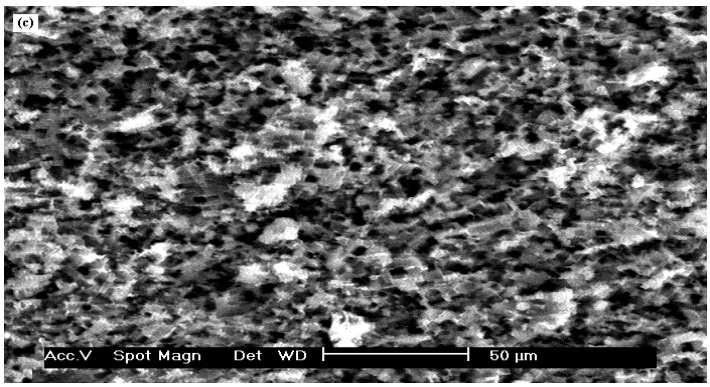

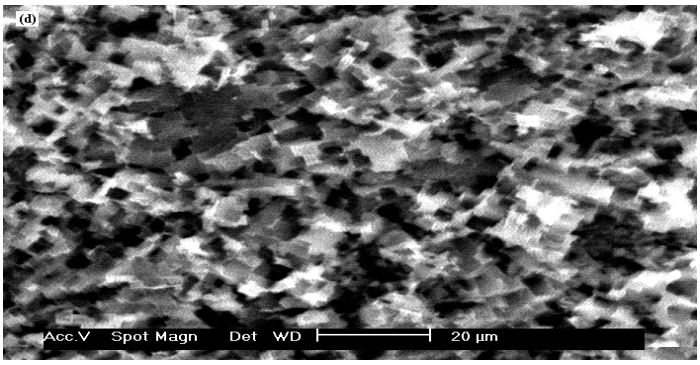

Fig.9 : SEM images of Al-Mg alloy surface after exposed to 2.0 M HCl solution with (a), (b) and without (c), (d) the addition of 0.5% BANPMB after 30 min.

3.5 Mechanism of inhibition

Many of the organic corrosion inhibitors are compounds with at least polar unit having atoms of nitrogen, sulfur, oxygen and in some cases selenium and phosphorous. The polar unit is regarded as the reaction centre for the adsorption process. In such a case the adsorption bond strength is determined by the electron density on the atom acting as the reaction centre and by the polarisability of the unit. Thus polar organic compounds acting as corrosion inhibitors are adsorbed on the surface of the bulk metal, M, forming a charge transfer from the inhibitor active sites and the metal:

$$M + RnX \leftrightarrow M : XRn$$

The size, orientation, shape and electric charge on the molecules determined the degree of adsorption and hence the effectiveness of the inhibitor.

The structure of BANPMB has three anchoring sites (one iminic group and two aromatic rings). Schiff base confers good protection and the compound when present in sufficient amount confer almost 99.0% protection of Al-Mg alloy in hydrochloric acid leads support this matter. The adsorption of the inhibitor obeys Langmuir adsorption isotherm (The plot of log $\theta/1-\theta$ vs log C_{inh} is linear). The increase in inhibiting efficiencies with the increase in the concentration of the studied Schiff base show that the inhibiting actions are may be due to that adsorption of the inhibitor molecules on the metal surface. It is generally assumed that the adsorption of inhibitor at the metal/solution interface is the mechanism of inhibitor through electrostatic attraction between the charged molecules and charged metal. BANPMB has been found to give an excellent inhibition due to the presence of the electron donating groups (such as $–OCH_3$), which increases the electron density on the nitrogen of the >C=N- group [55]. Thus leads to be the strong adsorption of inhibitor on the metal surface thereby resulting in high inhibition efficiency.

The free energy of adsorption (ΔG_{ads}) and heat of adsorption (Q_{ads}) are negative, suggest that the adsorption is physisorption which further supported from E_a values.

In presence of Schiff base with sufficient amount, both the cathoidc and anodic are polarized, but a tremendous polarization effect on the cathode. Thus, the Schiff base is mixed type inhibitor with a tremendous effect on the cathode.

The high efficiency of inhibitor may be traced to the presence of a methoxy ($–OCH_3$) group which exhibits a –I (inductive) effect and activated the benzene ring.

Conclusion

The present study leads to the following conclusions in controlling the corrosion of Al-Mg alloy by BANPMB in 2.0 M HCl.

1) The inhibition efficiency of the studied inhibitor, increase with increasing inhibitor concentration and decreases with increasing temperature.
2) The adsorption of the studied inhibitor obeys the Langmuir adsorption isotherm.
3) Thermodynamic parameters (ΔG_{ads}, Q_{ads} and E_a) show that the studied compound is adsorbed on Al-Mg alloy surface by exothermic, spontaneous and physical adsorption process.
4) BANPMB inhibits both cathodic and anodic reactions by adsorption but tremendous polarization effect on cathode and hence behave like mixed type inhibitor.
5) The obtained results about inhibition efficiencies from weight loss method, polarization study and electrochemical impedance spectroscopy are in good agreement with each other.

Acknowledgement : The authors are grateful to Chemistry Department, School of Sciences, Gujarat University, Gujarat, for the laboratory facilities. Two of the author Vidhi Panchal and Aesha Patel are also thankful to UGC-BSR for Research fellowship.

References

1. Li, X., Nie, X., Wang, L., Northwood, D.O. *Surf. Sci. Coat. Technol.* 200 (2005) 1994.
2. Sherif, E.M., Park, S.M. *Electrochim. Acta.* 51 (2006) 1313.
3. Quraishi, M.A., Rafiquee, M.Z.A. *J. Appl. Electrochem.* 37 (2007) 1153.
4. Ovari, F., Tomcsanyi, F., Turmezey, T. *Electrochim Acta* 33 (1988) 323.
5. Bentiss, F., Lagrenee, L. *J. Mater. Environ. Sci.* 2(10(2011) 13.
6. Hadi, Z.M., Alaa, S.K., Athir, M. *J. Mater. Environ. Sci.* 1(4)(2010) 227.
7. Ashassi-Sorkhabi, H., Shabani, B., Aligholipour, B. *Appl. Surf. Sci.* 252 (2006) 4039.
8. Khaled, K.F., Qahtani, M. *Mater. Chem. Phys.* 113 (2009) 150.
9. Maghraby, A.A.El. *The open corro. J.* 2 (2009) 189.
10. Khaled, K.F. *J. Appl. Electrochem.* 39 (2009) 2553.
11. Quraishi, M.A., Rafiquee, M.Z.A., Khan, Sadaf., Saxena, Nidhi *J. Appl. Electrocem.* 37 (2007) 1153.
12. Musa, A.Y., Mohamad, A.B., Kadhum, A.A.H., Tabal, Y.B.A. *Journal of Mater. Engin. and Perfor.* 20 (3) (2011) 394.
13. Bhat, I., Alva, V. *J. Indian Journal of Chem. Techn.* 16 (2009) 228.
14. Obot, I.B., Obi-Egbedi, N.O., Umoren, S.A. *Corro. Sci.* 51 (2009) 1868.
15. Yurt, A., Ulutas, S., Dal, H. *Appl. Surf. Sci.* 253 (2006) 919.
16. El-Dahan, H.A., Soror, T.Y., El-Sherif, R.M. *Mater. Chem. Phys.* 89 (2005) 260.
17. Emregul, K.C., Hayvali, M. *Corros. Sci.* 48 (2006) 797.
18. Chetouani, A., Hammouti, B., Benhadda, T., Daoudi, M. *Appl. Surf. Sci.* 249 (2005) 375.
19. Solmaz, R. *Corro. Sci.* 52 (2010) 3321.
20. Emregul, K.C., Kurtaran, R., Atakol, O. *Corros. Sci.* 45 (2003) 2803.
21. Gomma, G.K., Wahdan, M.H. *Mater. Chem. Phys.* 39 (1995) 209.
22. El-Rehim, S.S.A., Hassan, H.H., Amin, M.A. *Mater. Chem. Phys.* 78 (2002) 337.
23. Aytac, A., Ozmen, U., Kabasakaloglu, M. *Mater. Chem. Phys.* 89 (2005) 176.
24. Li, S.L., Chen, S., Lei, S.B., Ma, H., Yu, R., Liu, D. *Corros. Sci.* 41 (1999) 1273.
25. Wang, D., Li, S., Ying, Y., Wang, M., Xiao, H., Chen, Z. *Corros. Sci.* 41 (1999) 1911.
26. Bentis, F., Lagreene, M., Elmehdi, B., Mernari, B., Traisnel, M., Vezin, H. *Corrosion* 58 (2002) 399.

27. Yurt, A., Bereket, G., Ogretir, C. *J. Mol. Struct.: Theochem.* 725 (2005) 215.
28. Martinez, S. *Mater. Chem. Phys.* 77 (2002) 97.
29. Shah, N.K., Agrawal, Y.K., Talti, J.D., Shah, M.D., Desai, M.N. Schiff bases of ethyleneamine as corrosion inhibitors of zinc in sulphuric acid, Corro. Sci. 46 (3) (2003) 633.
30. Desai, M.N., Talati, J.D., Shah, N.K. *Indian J. of Chemistry*, 42A (12) (2003) 3027.
31. Talati, J.D., Desai, M.N., Shah, N.K. *Anti-Corro. Metho. and Mater*, 52 (2) (2005) 108.
32. Talati, J.D., Desai, M.N., Shah, N.K. *Mater. Chem. Phys.* 93 (1) (2005) 54.
33. Shah, M.D., Panchal, V.A., Mudaliar, G.V., Shah, N.K. *Anti-Corro. Meth. Mater*, 58 (3) (2011) 125.
34. Rezaei, F., Sharif, F., Sarabi, A.A., Kasiriha, S.M., Rahmaniam, M., Akbarinezhad, E. *J. Coat. Technol. Resea.*, 7 (2010) 209.
35. Zhou, Q., Wang, Y., Bierwagen, P. *Corro. Sci.*, 55 (2012) 97.
36. Wang, X., Yang, H., Wang, F. *Corros. Sci.*, 55 (2012) 145.
37. Shah, M.D., Patel, A.S., Mudalliar, G.V., Shah, N.K. *Portugaliae Electrochimi. Act.* 29 (2) (2011) 101.
38. Hosseine, M.G., Mertens, S.F.L., Gorbani, M., Arshadi, M.R. *Mater. Chem. Phys.* 78 (2003) 800.
39. Umoren, S.A., Obot, I.B., Akpabio, L.E., Etuk, S.E., *Pigment Resin Technol.* 37 (2) (2008) 98.
40. Umoren, S.A., Obot, I.B., Ebenso, E.E., *E-Journal Chem.* 5 (2) (2008) 355.
41. Tang, L., Li, X., Li, L., Mu, G., Liu, G. *Surf. Coat. Technol.* 201 (2006) 384.
42. Lebrini, M., Lagrenée, M., Vezin, H., Gengembre, L., Bentiss, F. *Corros. Sci.* 47 (2005) 491.
43. Khairou, K.S., El-Sayed, A. *J. Appl. Polym. Sci.* 88 (2001) 866.
44. Zhang, Q.B., Hua, Y., *Matar. Chem. Phys.* 119 (2010) 57.
45. Joseph, B., John, S., Joseph, A., Narayana, B. *Ind. J. of Chem. Technol.* 17 (2010) 366.
46. Founda, A.S., Abd El-Aal, A., Kandil, A.B. *Desalination.* 201 (2006) 216.
47. Umoren, S.A., Ebenso, E.E. *Mater. Chem. Phys.* 106 (2007) 393.
48. Umoren, S.A., Obot, I.B., Ebenso, E.E. *E-Journal Chem.* 5 (2) (2008) 355.
49. Desai, M.N., Talati, J.D., Shah, N.K., *Anti-Corros. Metho. and Mater.* 55 (2008) 27.
50. Bentiss, F., Lebrini, M., Lagrenee, M. *Corros. Sci.* 47 (2005) 2915.
51. Machnikova, E., Whitmire, K.H., Hackerman, N., *Electrochim. Acta* 53 (2008) 6024.
52. Gunasekaran, G., Chauhan, L.R. *Electrochim. Acta.* 49 (2004) 4387
53. Bockris, J.O.M., Yang, B. *J. Electrochem. Soc.* 139 (1991) 2237.
54. Hassan, H.H., Abdelghani, E., Amin, M.A. *Electrochim. Acta* 52 (2007) 6359.
55. Agrawal, Y.K., Talati, J.D., Shah, M.D., Desai, M.N., Shah, N.K., *Corros. Sci.* 46 (2004) 633.